Neutron Noise Observations in German KWU Built PWR and Analyses with the Reactor Dynamics Code DYN3D

Rohde, U.; Seidl, M.; Kliem, S.; Bilodid, Y.;

Originally published:

November 2017

Annals of Nuclear Energy 112(2018), 715-734

DOI: https://doi.org/10.1016/j.anucene.2017.10.033

Perma-Link to Publication Repository of HZDR:

https://www.hzdr.de/publications/Publ-25370

Neutron Noise Observations in German KWU Built PWR and Analyses with the Reactor Dynamics Code DYN3D

Ulrich Rohde
HZDR-Innovation Rossendorf
P.O. Box 510119, D-01314 Dresden, Germany
u.rohde@hzdr.de

Marcus Seidl
PreussenElektra GmbH
Tresckowstrasse 5, 30457 Hannover, Germany
marcus.seidl@eon.com

Sören Kliem
Helmholtz-Zentrum Dresden - Rossendorf,
Reactor Safety Division,
P.O. Box 510119, D-01314 Dresden, Germany
s.kliem@hzdr.de

Yurii Bilodid
Helmholtz-Zentrum Dresden - Rossendorf,
Reactor Safety Division,
P.O. Box 510119, D-01314 Dresden, Germany
y.bilodid@hzdr.de

ABSTRACT

Low-frequency neutronic noise with a bandwidth of up to ten percent of the reactor power has been observed in Konvoi-type PWRs in Germany in the last years. Several attempts were made to identify the reasons for increased magnitudes of the neutronic fluctuations in comparison with pre-Konvoi reactors, and various hypotheses have been created to explain this effect.

In this paper, results of noise simulations performed with use of the reactor dynamics code DYN3D are presented. Both fluctuations of the coolant inlet temperature and mass flow rate were considered. Besides of un-correlated fluctuations, correlated temperature fluctuations were simulated. The correlations between fluctuations in the individual fuel assemblies were obtained based on an experimentally validated coolant mixing model. However, the features of the neutronic noise found in the simulations do not correspond to the measurements.

Obviously, more complex mechanisms than only temperature and/or mass flow fluctuations have to be considered. Simulated fluctuations of the local moderator density, independently from thermal hydraulics, indicate that potentially deformations or vibrations of the fuel rod lattice leading to variations of the local moderator content might be responsible for the observed neutronic noise. Advanced models coupling neutronics, thermal hydraulics, turbulence and mechanical modelling have to be developed.

KEYWORDS
PWR, KWU, NEUTRON NOISE, DYN3D

1. INTRODUCTION

For a chain-reacting pile Weinberg already investigated the characteristics of neutron noise driven by an oscillating neutron absorber in 1948 (Weinberg and Schweinler, 1948). The early research focus was on relatively small research reactors such as the ORR and the HFIR which can be treated well using the point kinetic approximation (Robinson, 1967). Analysis mainly focused on a superposition of reactivity fluctuations due to a combination of white inlet temperature fluctuations and control rod vibrations excited by turbulent flow.

All of the following remarks concern KWU built PWRs in Germany. They were designed by Kraftwerk Union AG (KWU) under the names "Vor-Konvoi" and "Konvoi" line of pressurized water reactors in the 1980s and 1990s. These 1300 MWe type of plants all feature a four-loop primary coolant cycle, 193 fuel assemblies and a cold core height of 390 cm. From the neutronics perspective Vor-Konvoi and Konvoi plants have very similar properties with an average power density of about 37 W/gU.

In these plants neutron noise was utilized as part of a recurrent maintenance procedure to check the position of certain eigen-frequencies in the APSD (auto-spectral power density) measured by in-core and ex-core neutron detectors. These eigen-frequencies were tied to characteristic mechanical movements of the reactor core's components: oscillations of the pressure vessel, relative movements of the core barrel versus the pressure vessel, eigen-mode oscillations of the fuel assemblies or oscillations of the core's lower plenum structure (Seidl, 2015; Fiedler, 2002; DIN 25475-2, 2009).

Some basic assumptions concerning the APSDs were always taken as granted. First, it has been assumed that the mechanical movements of the core components do not couple back to the flow of the moderator through the core. Second, it was always well known that the main contribution to the neutron noise were not the above mentioned oscillations but the continuous, low frequency part of the APSD. This contribution quickly decays between about 0.5 and 10 Hz over several orders of magnitude (Grondey, 1992). It makes up more than 95% of the total signal. Frequencies below 0.5 Hz in principle also belong to the low frequency neutron noise (LFNS) but are usually disregarded because of potential contributions from reactor controls during measurement.

The LFNS has always had two characteristics which were difficult to explain: a near 180° phase relationship between opposing ex-core and in-core neutron detectors (i.e. in core quadrant 1 and 3 or 2 and 4) and near simultaneous occurrence of peaks and troughs along axial detector string (Grondey, 1992).

The purpose of this paper is to comment on the potential explanations for a recent period of increase and decrease of neutron noise s in KWU-type PWRs. No classical explanation of the potential sources of neutron noise (i.e. power or enrichment uprates, increase in burnup, core composition or core loading strategy) alone has so far been able to explain the observations. In section 2 the classical theoretical understanding is summarized. In sections 3 and 4 calculations with DYN3D are shown, explaining that classical explanations are not able to fully explain recent observations. In section 5 the case for a further development of core simulation tools is made.

2. THEORETICAL UNDERSTANDING OF NEUTRON NOISE IN KWU BUILT REACTORS

If one considers a point reactor with core parameters typical of a PWR it can be seen that in the frequency range between 0.5 and 10Hz the zero power transfer function is almost constant. As a result the structure of the observed APSD in this range is a mirror image of the characteristics of the point reactor's external noise source. For example, if in this frequency range a white noise source would perturb the point reactor, the resulting APSD would also be almost flat in this range. If the external noise source like a vibrating mechanical structure has a characteristic eigenfrequency, the this frequency would again be seen as a distinctive peak in the APSD (Seidl, 2015).

Traditionally the LFNS scaled proportionally to the change of the moderator temperature coefficient during a cycle. This meant that the neutron noise amplitude approximately doubled from BOC to EOC during the standard one year cycles. Early on this resulted in the conclusion that fluctuations in the core inlet temperature were mainly responsible for the LFNS at full power.

Two conditions need to be met in order to explain the LFNS: the core inlet temperature distribution under steady state conditions needs to be inhomogeneous and the relative position (with respect to the fuel assemblies) of this distribution has to change over time.

This conclusion was drawn in part because the sum of the neutron noise signals from all four core quadrants cancels out to a high degree in the reactors and therefore the average, core-wide inlet temperature fluctuation is expected to be very small. On the other hand if the inlet core temperature fluctuations would occur independently at each assembly location the total reactor power would be expected to fluctuate noticeably, too (which is not the case).

The magnitude of the LFNS in a Konvoi plant at BOC historically has been about 1% while at a Vor-Konvoi plant it was about 3%. These values refer to the peak-to-peak full signal width of the unfiltered neutron noise signal in relation to its DC level. Noise contributions from detection and amplification sources have been found to be negligible.

However, there was no obvious reason why the core inlet temperature distribution should fluctuate more strongly in Vor-Konvoi than in Konvoi plants. By rule of thumb it was concluded at the time that both the feed water preheaters in the steam generators of the Vor-Konvoi plants and the lack of a dedicated structure for flow mixing in the lower plenum of these plants did induce bigger position fluctuations and bigger gradients of the core inlet temperature distributions compared to the Konvoi line. The reason for the stronger temperature gradients was believed to be due to the preheater design in which the outermost steam generator tubes are cooled more than average and thus is adding to the temperature gradient across the cold legs. Since the plants lack any temperature measurement instrumentation at the bottom nozzle of the fuel assemblies this explanation stood unchallenged for the next 20 years.

Recently, several theoretical analyses of neutronic noise induced by coolant inlet temperature and mass flow rate fluctuations in Konvoi an Pre-Konvoi type PWR were performed. In (Bermejo, 2017), results of simulations of neutronic noise in the Spanish Trillo NPP using the S3K code are reported about. The Trillo reactor combines elements of Konvoi and Pre-Konvoi reactors (Secondary Core Support Structure SCSS and Flow Distribution Device FDD), what is important with respect to coolant mixing in the lower plenum of the reactor. The impact of mixing was investigated in the simulations. Results of the simulations are compared with an analytical model and data from the NPP. It was concluded, that the observations cannot fully be explained. Probably, the influence of mechanical vibrations has to be considered.

In (Bläsius, 2016) a comprehensive overview on observations in German PWR is provided. Advanced analytical models have been developed and applied to understand qualitatively the features of the observed neutronic noise. The authors of this report came also to the conclusion, that considering only thermo-hydraulic effects, the observations can hardly be explained in detail. Coupling of neutronics with mechanical, and may be, more sophisticated thermos-hydraulic models taking into account cross flow in the reactor core, is suggested.

3. VERIFICATION OF CLASSICAL KNOWLEDGE WITH DYN3D

3.1 The DYN3D code

In the past, very often analytical approaches were used to analyze the behavior of LFNS in dependence from noise sources like temperature, mass flow rate or pressure fluctuations in the reactor core. The corresponding reactor parameters like moderator temperature, mass flow rate or boron concentrations are split into a constant or smoothly changing (fundamental) part and a stochastically fluctuating part. Putting these ansatzes into the balance equations, after linearization and performing Fourier or Laplace transformation, one gets algebraic equations for the fluctuating parts in the frequency domain.

As a result, we obtain frequency-dependent transfer functions $F(\omega)$ between e.g. stochastic fluctuations of the temperature δT and neutronic signals δN, which can represent the global reactor power Q or, for example, local linear heat rate (LHR) q'_{local}:

$$F(\omega) = \delta N(\omega) / \delta T(\omega),\ N = Q \text{ or } q'_{local} \qquad \text{(Equ. 1)}$$

To get these transfer functions between fluctuations of thermo-hydraulic parameters like moderator temperature or mass flow rate, we performed numerical simulations in the time domain using the reactor dynamics code DYN3D.

DYN3D (Rohde, 2016; Kliem, 2016; Bilodid, 2016) is a simulation tool for transients in LWR, which has been developed in Helmholtz-Zentrum Dresden-Rossendorf (HZDR) over many years. The 3D multi-group neutron kinetics model is based on nodal expansion methods for the neutron flux calculation in various core geometries (Cartesian, hexagonal or on a trigonal grid, Grundmann, 1999 and Duerigen, 2013).

Besides neuron kinetics, DYN3D includes a four-equation thermo-hydraulic model for parallel channels without crossflow between them, a boron transport model, and a fuel rod model. The fuel rod model comprises the solution of the one-dimensional heat conduction equation and the thermo-mechanical modelling of the gas gap between fuel and cladding (Rohde, 2001).

By applying this code, transients can be simulated which are caused by the following external perturbations:

- Movement of control rods or groups of them
- Variations of the coolant inlet temperature and/or boron concentration at the core inlet (separately at each fuel element position)
- Changes of the pressure drop over the core or of the core mass flow rate
- Variations of the coolant pressure

In the stand-alone version of the code, these perturbations can be given in the form of time tables in the input of DYN3D.

Using this code, transient simulations were performed calculating the global reactor power and local LHRs caused by fluctuations of the core inlet temperature or mass flow rate. These fluctuations were given as input function time tables, which were produced by a noise generator. As a basic hypothesis, white noise was assumed. The transfer function according to equation (1) was obtained by performing a Fast Fourier Transformation (FFT) of the global reactor power or LHR at different positions. The local LHR values are interpreted as neutron detector readings that mean, the transfer behavior of the detector itself is neglected.

The features of the calculated transfer functions like frequency characteristics, maximum magnitudes and phase shift, are then compared to the measured characteristics to conclude about possible causes for the neutronic noise.

3.2 Scope of the simulations

Using the DYN3D code, reactor noise simulations were performed considering different possible mechanisms for the generation of noise. First of all, classical LFNS was simulated assuming stochastic fluctuations of the coolant or moderator temperature at the core inlet.

Besides of temperature induced noise, neutronic fluctuations caused by stochastic variation of the mass flow rate and by independent variations of the moderator density were considered. The aim of the simulations was, on the one hand, to assess qualitatively the characteristics of the transfer functions in the frequency domain, on the other hand the magnitudes of the neutron flux fluctuations, related to a normalized magnitude of the perturbation.

Besides of uncorrelated fluctuations of the temperature at the inlet of each individual FA, correlated fluctuations were considered. Uncorrelated fluctuations could be caused by turbulence of the coolant flow in the lower plenum which propagates to the core inlet. If we assume fluctuations of the cold leg temperatures in the loops, correlations between the fluctuations at each FA inlet appear, because each loop affects more or less all FA allocated to a sector of the core connected with one of the loops. A physical model based on experimental data was developed and applied to assess the correlation between temperature fluctuations in the FA.

Based on the characteristics of the neutron noise it was assessed, if one of the considered noise sources can be identified to explain the observed neutronic fluctuations.

3.3 Initial and boundary conditions

The DYN3D calculations on neutron noise simulation were performed for a generic Konvoi reactor core with MOX loading. Figure 1 shows the core loading scheme.

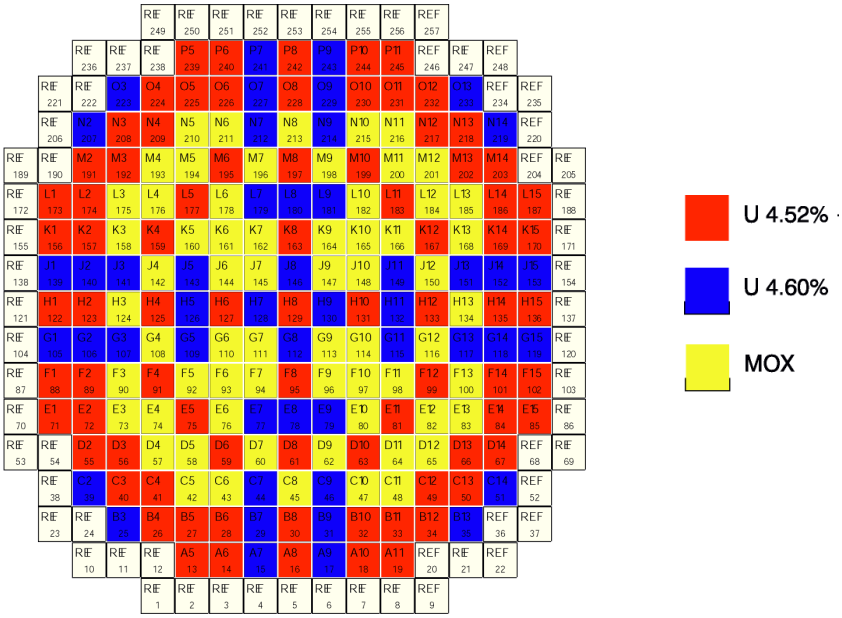

Figure 1: Core loading scheme of a generic MOX core of a Konvoi type reactor (129 UO_2 and 64 MOX fuel assemblies; Kliem, 2004)

All calculations were performed for close to EOC conditions (with a critical boron concentration of 50 pcm), because the absolute value of the moderator density coefficient of the reactivity is maximal at these conditions. Therefore, maximum noise amplitudes are generated by moderator temperature fluctuations.

The main core parameters are:

- Thermal reactor power Q_{th} = 4000 MW
- Coolant inlet temperature T_{in} = 293.4 ^{o}C
- Core mass flow rate 20077 kg/s (including 6 % core bypass flow)

From steady state core calculations by DYN3D, the following reactivity parameters were obtained (table 1).

Reactivity effect	Unit	Value
Moderator density $\delta\rho/\delta\rho_{mod}$	pcm/kg m^{-3}	30.0
Moderator temperature $\delta\rho/\delta T_{mod}$	pcm/K	3.29
Total temperature effect (including density change) $\delta\rho/\delta T_{tot}$	pcm/K	-71.9
Fuel temperature (Doppler effect) $\delta\rho/\delta T_{fuel}$	pcm/K	-2.78

Table 1: Reactivity coefficients calculated by DYN3D for the generic core loading

3.4. Uncorrelated temperature fluctuations

Method of analysis

In our simulations, the coolant temperature at the core inlet was assumed to be overlapped by stochastic fluctuations. In (Bläsius, 2016) a formula is referred to which gives a frequency dependency of the APSD of quantities transported within a fluid flow. According to this formula, the APSD of the temperature fluctuations depends from the frequency f of the fluctuating modes by

$$APSD\ (f) \sim \left[1 + \left(\frac{f}{f_0}\right)^2\right]^{-\frac{5}{6}}$$

This formula represents the fact that fluctuations of transported quantities in a turbulent flow are increasingly dissipated at higher frequencies. f_0 is the characteristic frequency at which the dissipation becomes relevant. The function shows a smooth behavior over frequency with rapid decrease at frequencies above 0.1 Hz and thus does not induce peaks or resonances in the interesting frequency range.

Therefore, for simplicity we assume in our simulations white noise. White noise means, that the magnitude of the fluctuation is chosen randomly for each time point in-between a given interval around the mean value, independently from the choice at previous and next time point. The probability distribution for the selection of the random value must be the same for each time point. In this way, DYN3D input tables were generated for the coolant inlet temperature.

In the first case, we consider un-correlated temperature noise that means the fluctuations of the temperature at each fuel assembly position are independent from the fluctuation at other positions. This might be justified in the case of local turbulent fluctuations in the coolant flow.

Figure 2 shows, for example, a simulated white noise signal with a maximum magnitude of the fluctuations of $\pm$ 5K with a time step of 10 ms.

A magnitude of 5 K for the temperature fluctuations can be considered as a conservative estimate. It seems to be difficult to imagine any physical or technical mechanisms which could initiate such strong temperature fluctuations. However, assuming linearity of the noise, the magnitudes of the neutronic fluctuations can be scaled to any magnitude of the temperature fluctuations.

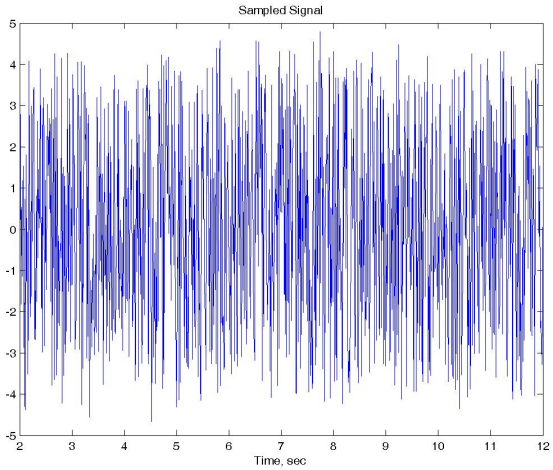

Fig. 2: Temperature noise at a single fuel assembly position with a magnitude of $\Delta T = \pm$ 5K

Fig. 3 demonstrates the corresponding fluctuation of the reactor power in the time domain.

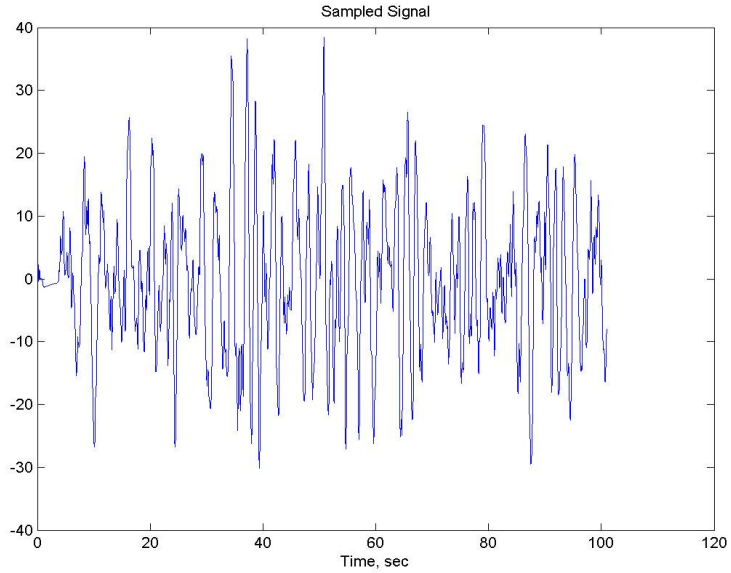

Fig. 3: Reactor power fluctuations (units of MW) caused by temperature noise in Fig.2

We observe some power bursts of up to about 40 MW within stochastically varying intervals of about 10 – 20 s.

Figure 4 shows APSD of the global reactor power obtained from a DYN3D calculation over 100 s of process time with a time step of 50 ms in a logarithmic scale. This calculation was performed with a magnitude of the temperature fluctuations of 1.5 K.

The APSD function is obtained from the time behavior of the reactor power, calculated by DYN3D, by applying Fast Fourier Transformation (FFT). It is normalized in this way that the values correspond to the magnitudes of the power fluctuations, related to a frequency interval of 1 Hz (MW/Hz). For the performance of FFT we used an excel tool available from the internet and adopted for our purposes (Debevec, 2006; Kerr, 2009).

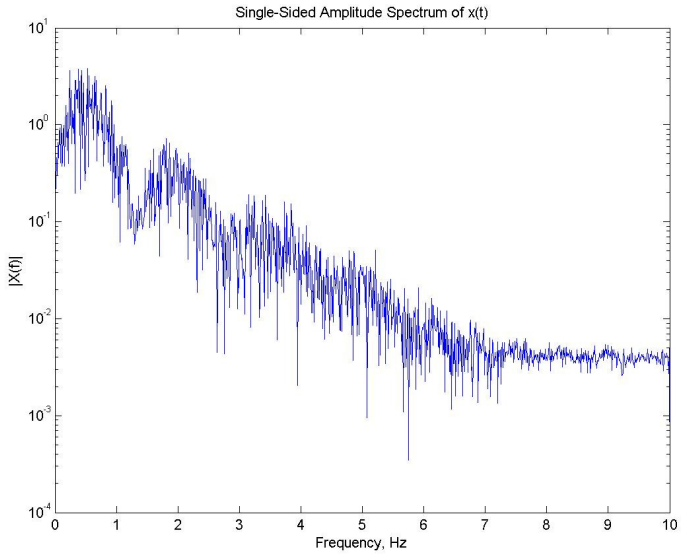

Fig. 4: Auto Power Spectral Density of the global reactor power in the case of uncorrelated white temperature noise with a magnitude of ± 1.5 K

According to the sampling theorem $f_{max} = 1/(2*\Delta t)$ (Liewers, 1985), the time step of the simulation (availability of discrete power values) defines the frequency interval for the resulting APSD function (in our case 10 Hz). The number of time steps corresponds to the number of frequency modes from the FFT analysis. The more frequency modes are included, the more accurate is the FFT.

As mentioned above, for temperature induced LFNS only the frequency range up to about 5 Hz is sufficient (Runkel, 1987). That's why for temperature noise, the analysis of the APSD spectra will be limited in the following to the frequency interval up to 5 Hz.

In the numerical simulation small and slow drifts of the average power after switching from steady state to transient solution of the equations can occur. Such a long term drift can be induced in reality by inherent features of the system like thermal hydraulics feedback, or in numerical simulation by small inconsistencies between steady state and transient calculation.

To eliminate this effect, the basic signal (calculated reactor power) was processed in this way, that the long-term averaged value was subtracted from the actual, fluctuating signal, and only the difference, representing the real noise signal, was analyzed.

The long-term averaged signal is calculated as,

$$\overline{N}(t) = \frac{1}{t}\int_0^t N(\tau)\cdot d\tau \qquad \text{(Equ. 2a)}$$

where N represents the reactor power or the local neutronic signal.

The compensated fluctuation is then $N_{comp}(t) = N(t) - \overline{N}(t)$ (Equ.2b)

Moreover, to make the qualitative analysis of the APSD spectra more demonstrative (in particular, to determine resonance frequencies), they were smoothed by applying a gliding average over the last five values. Figure 5 shows the smoothed APSD spectrum of the reactor power for uncorrelated temperature noise (same case as shown in Fig. 4).

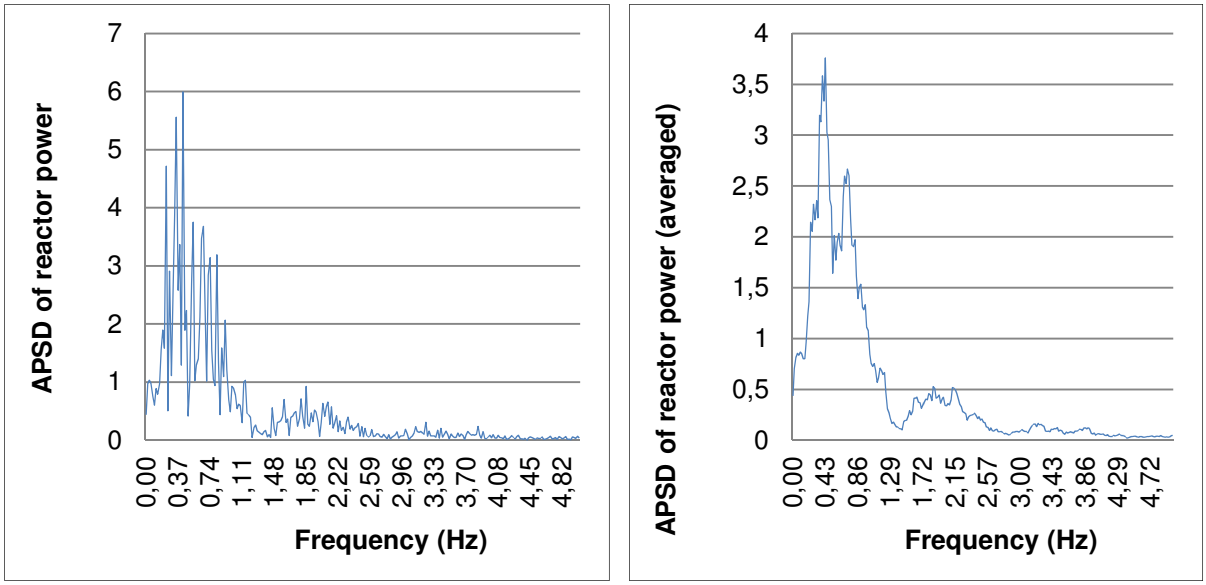

Fig. 5 APSD of the reactor power (right – smoothed)

For all simulations described in the following, signal analysis was performed in the way as described above – smoothing by gliding averaging and separation of the long-term drift component from the neutronic signals.

The APSD spectra are used to get qualitative information about the noise, like information about dominating frequencies (resonances), damping over frequency and damping over axial height (for local noise signals).

Besides of the frequency behavior, the effective magnitude of the neutronic noise was determined as the mean square magnitude of the neutronic signal (global power or local LHR) in the time domain.

Moreover, cross-correlation functions were considered. The cross correlation function for discrete signals is defined as (Liewers, 1985):

$$corr(k) = \frac{\sum_{i=1}^{N} x[i] \cdot y[i+k]}{\sqrt{\sum_{i=1}^{N} (x[i])^2} \cdot \sqrt{\sum_{i=1}^{N} (y[i+k])^2}} \qquad \text{(Equ. 3)}$$

x_i and y_i are the values of the signal at discrete time points i = 1,…N (t0+Δt, …t0+i · Δt , t0+N · Δt), k corresponds to a time shift between the signals of the interval τ in multiples of Δt. The cross correlation function can have a maximum value of unity. In this case, the time signals are fully correlated. Cross correlation values of about < 0.2 can be considered as statistically not relevant.

Results of simulations

The simulation of temperature induced noise as described above (see Fig. 4 and 5) is considered as the basic case. The process time considered was T = 100 s, the time step Δt = 0.05 s. The frequency interval covered by this analysis is 10 Hz according to the Nyquist theorem. For the FFT in the standard case we have used 1024 data points. The FFT algorithm by Cooley and Tuckey (1966) used by us requires a number of 2^n data points.

In the results shown on figures 4 and 5 we can see a resonance of the APSD at about 0.45 Hz. At higher frequencies, the APSD function decreases rapidly.

The effective magnitude of the reactor power fluctuations was determined as normalized root mean square (NRMS) deviation from the power compensated by the long-term drift (see equ. 2). For comparability, we related the fluctuation magnitudes always to the steady state value Q_0 and to 1K of temperature fluctuation. For the considered basic case we obtained a value of about 0.20 % of the steady state initial value per degree of temperature fluctuation (% K^{-1}) corresponding to value of 8.0 MW. The maximum peak-to-peak magnitude of power fluctuations reaches up to 1.2 % K^{-1}. This is due to single power bursts (see Fig. 3) which occur perhaps by stochastic correlations between the local fluctuations.

Besides of the APSD of the total reactor power, the APSD of the linear rod power of the fuel element No 29 being the hottest FE in the reactor were considered at two different axial positions: z = 45 cm and z = 315 cm from the lower boundary of the core.

Figure 6 shows those APSD. The resonance frequencies for the local parameters are about the same as for the reactor power (between 0.4 and 0.8 Hz). There are some secondary peaks, which could not fully be explained. Local fluctuations are, related to the average value, about a factor of 2 stronger than fluctuations of the global reactor power (0.4 % K^{-1}). The maximum magnitudes of the fluctuations reach 2 – 2.5 % K^{-1}.

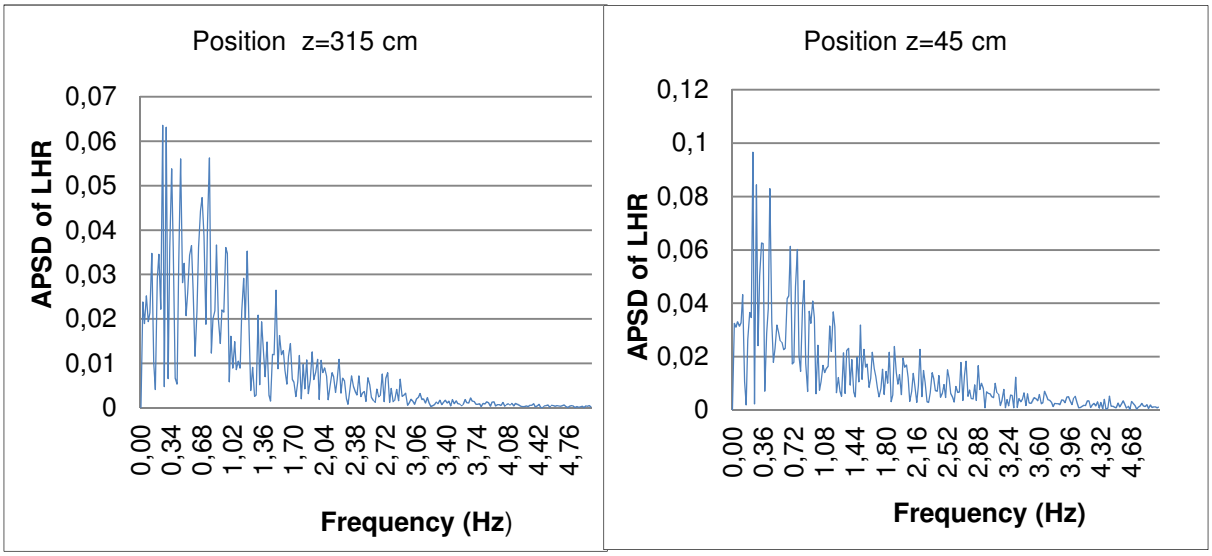

Fig. 6: APSD of the linear heat rate in channel 29 at position z = 45 cm (left) and z = 315 cm (right)

From figure 6 we can see, that the magnitude of the noise decreases with axial height, what is in correspondence with the theory.

For the local signals, we look additionally at the cross correlation functions (see equation 3). The upper graphics in figure 7 shows the cross correlation function between two different positions of the same FA (number 29) in dependence from the time shift τ (in s), the lower picture presents the CCF between locations at the same axial position (z = 45 cm), but between different FA (number 29 and 35).

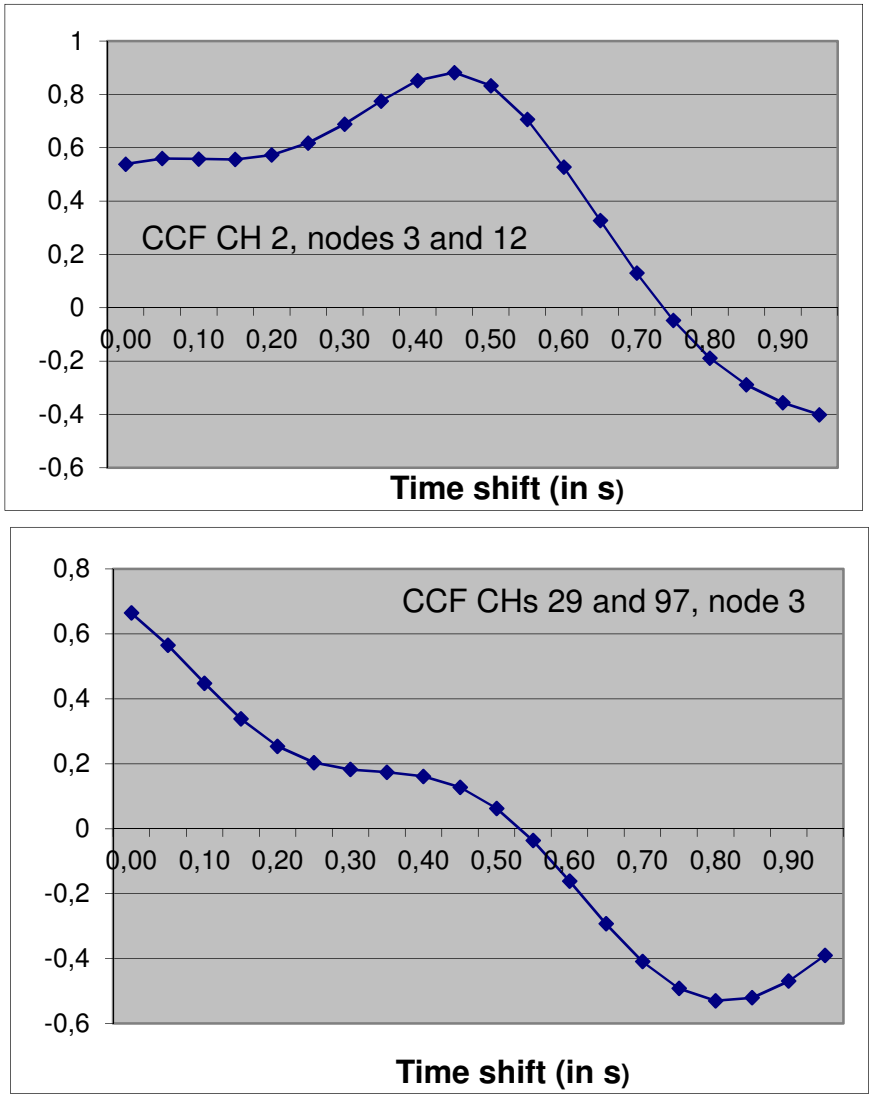

Fig. 7: Cross correlation function between in dependence from the time shift

Upper: CCF between two positions (at z = 45 cm and 315 cm) of the same FA, lower: CCF for the same axial position (z = 45 cm) of two different FA (numbers 29 and 97)

The CCF between two axial positions of the same FA shows a maximum of about 0.88 for a time shift of about 0.5 s. That means there is a high degree of correlation between the two signals, one of them shifted by 0.5 s. This time shift corresponds to the transport time of the coolant between the two axial positions. However, this time shift was not found in the measurement signals. The measurement signals show a high degree of correlation between all axial positions in the same FA, a phase or time shift was not observed.

The degree of correlation between signals from two different FA at the same axial position, however, does not have a clear maximum corresponding to the transport time. There is a relevant correlation (CCF of about 0.6), that means, the signals from different (not neighboring) FA are correlated to some degree what is assumed to be caused by the global fluctuations of the reactor power.

Impact of numerics

In the simulations, the impact of numerical parameters like time step and time interval for the noise simulation, was considered. The following items have to be taken into account:

- Sufficient statistics for the fluctuations should be ensured. That means, a sufficiently long time interval of white noise should be calculated. Process times of 100; 500 and 1000 s were considered.
- For minimization of the numerical diffusion, the Courant criterion should be considered. The numerical diffusion is minimal, when the Courant criterion r is close to unity:

$$r = w \cdot \Delta t / \Delta z$$

  W is the velocity of coolant flow, Δt is the time step and Δz represents the axial mesh size. With w ~ 5 m/s and Δz ~ 0.30 m we get a recommended time step width of about 0.05 s with respect to numerical diffusion. However, the fulfilling of the Courant criterion is not a condition with respect to the stability of the numerical scheme used in DYN3D. The scheme is unconditionally stable.

- The sampling theorem must be considered. For a frequency interval of 5 Hz, a time step size of 0.1 s is sufficient. However, to cover broader frequency intervals, smaller time steps are required.

In the code DYN3D, a very low diffusive numerical scheme is implemented for the solution of the enthalpy balance equation for the coolant enthalpy (U. Grundmann et al. 2005). The energy conservation equation can be presented in the characteristic form of a hyperbolic partial differential equation,

$$\frac{\partial y}{\partial t} + u\frac{\partial y}{\partial z} = q \qquad \text{(Equ. 4)}$$

where y is the unknown variable (in our case enthalpy) and q is the source term for coolant heating.

The method is based on a combination between the method of characteristics (MOC) and the second order Lax&Wendroff scheme (Richtmyer, 1967).

The method of characteristics can be illustrated by the scheme shown in Fig. 8. A fictive fluid particle is tracked on its way within one time step Δt. The subscript describes the time step, while the superscript characterizes the axial node level within a coolant channel. Over one time step, the particle moves from position y* to y_i^n. If the Courant criterion is exactly equal to 1, y* corresponds to y_{i-1}^{n-1}. In this case, we have no numerical diffusion. However, it is not possible to generally fulfill the condition r = 1, because on the one hand, the coolant velocity varies in space and time, and on the other hand, the thermo-hydraulics time step is controlled by other, independent criteria. If r is not equal to unity, the value y* at the basis of the characteristic line has to be interpolated between neighboring values as shown in the scheme, what leads to numerical diffusion. The numerical diffusion is the higher; the more far from 1 is r.

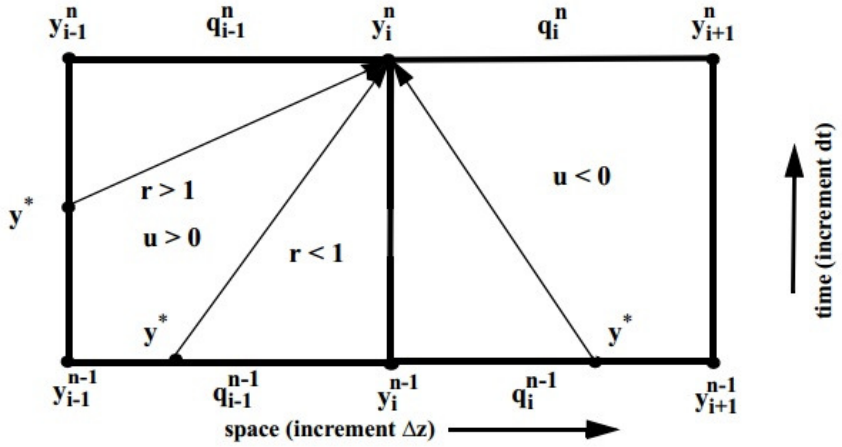

Fig. 8: Illustration of the Method of Characteristics
(from Grundmann, 2005)

Alternatively, we could choose a second order numerical scheme using not only first order, also second order derivatives and connecting the three values y_{i-1}^{n-1}, y_i^{n-1} and y_{i+1}^{n-1} to calculate y_i^n.

Such kind of scheme is the Lax&Wendroff scheme. It is of higher order of accuracy than the MOC in the general case (r not equal to 1), but only conditionally stable for r < 1. This would put additional restrictions on the time step size.

Based on these considerations, a combination of the MOC with the Lax&Wendroff scheme was implemented which is illustrated in Fig. 9.

At the basis of the characteristic, that means, the way of a fictive fluid particle over one time step, the Lax&Wendroff scheme is used in correspondence with r < 1. Then, within each node (if the particle moves over more than one node within a time step), the MOC is used with exactly r = 1 from step to step.

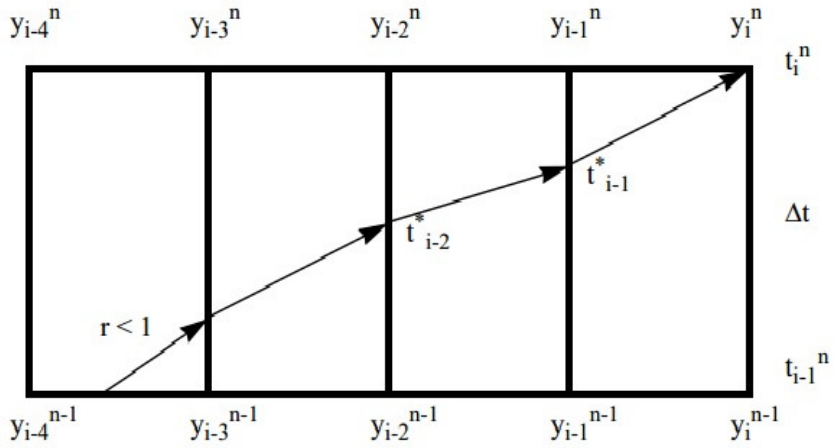

Fig. 9: Illustration of the combination between Method of Characteristics and Lax&Wendroff scheme
(from Grundmann, 2005)

By combining both schemes in the way described above, we obtain a numerical procedure with high accuracy and minimized numerical diffusion.

For numerical tests, calculations with the following combinations of numerical parameters were performed:

A. T = 100 s; Δt =0.02 s;

B. T = 100 s; Δt = 0.05 s;

C. T = 100 s; Δt =0.1 s;

D. T = 500 s; Δt = 0.1 s.

Another parameter influencing the calculated APSD spectrum is the number of FFT modes or frequency points.

The reference case as described above is the case B. Fig. 10 and 11 show the APSD for the cases A and C with the same number of 1024 modes (compare with figure 4 left).

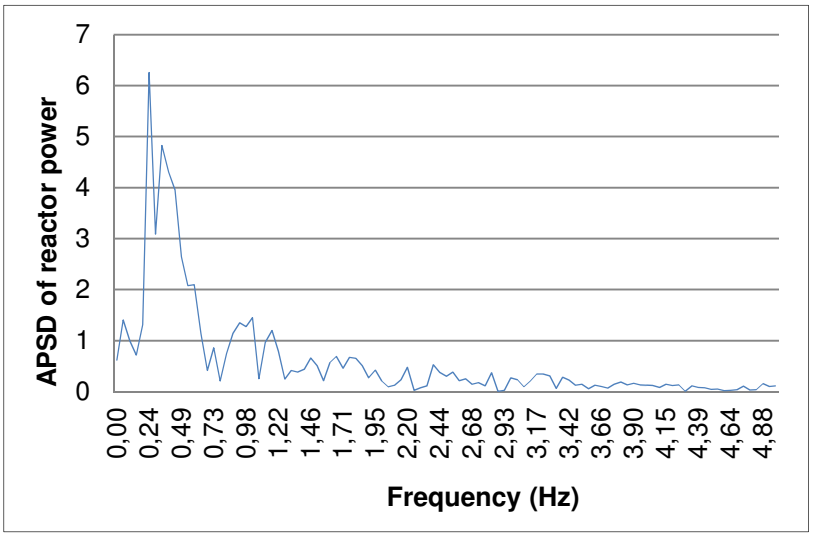

Fig. 10: APSD of the reactor power with time step size Δt = 0.02 s (case A)

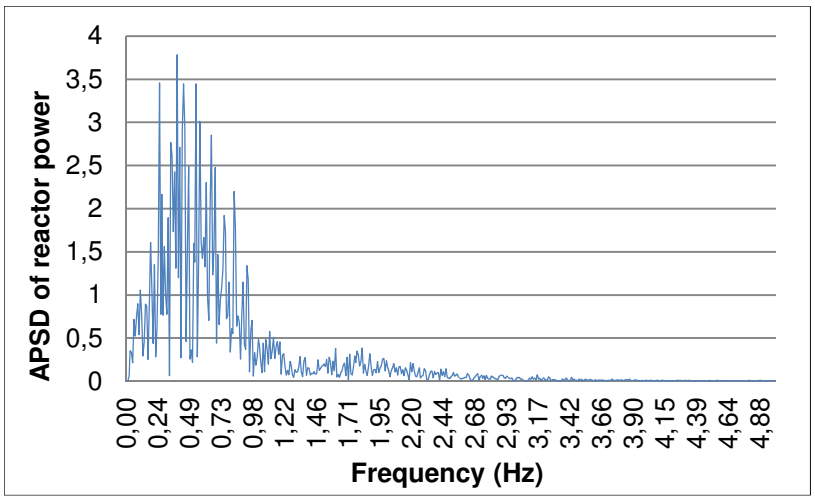

Fig. 11: APSD of the reactor power with time step size Δt = 0.1 s (case C)

The structure of the spectrum is more pronounced in case C then in case A, because the Nyquist frequency is lower in case C, and with a fixed number of FFT modes we have more frequency points within the frequency interval of 5 Hz.

Figure 12 shows the APSD for the case B simulation with different numbers of FFT frequency modes.

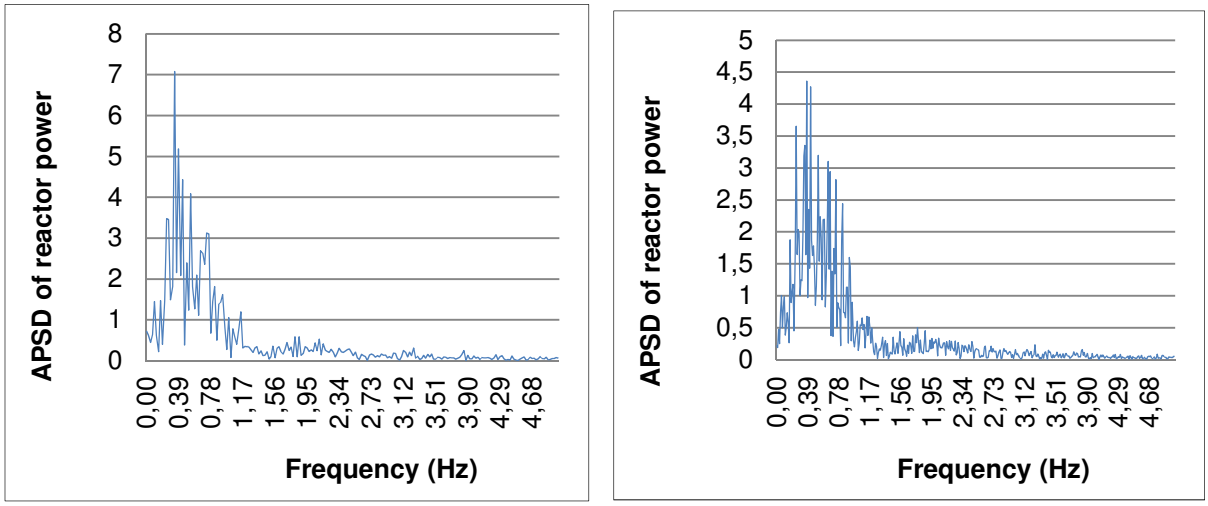

Fig. 12: APSD of the reactor power with time step from case B simulation with N = 2048 left) and N = 4096 modes (right)

Further, a simulation with the same parameters as case C ($\Delta t = 0.1$ s) was performed over a longer process time of 500 s. Using the same number of frequency modes, the APSD spectrum is identical to that of case C. However, the statistics for the determination of the mean square and maximum fluctuation amplitudes is better.

An overview on the impact of numerical and FFT parameters is given in table 2.

Case	Numerical parameters	NP	ΔQ_{max} [% K^{-1}]	Sigma [% K^{-1}]	f_{res}
A	$\Delta t = 0.1$, T=100 s	1024	1.04	0.181	0.45
B	$\Delta t = 0.05$, T = 100 s	1024	1.15	0.200	0.44
		2048			0.44
C	$\Delta t=0.02$, T = 100 s	1024	1.02	0.181	0.44
		2048			0.44
		4096			0.38
D	$\Delta t=0.1$ s, T=500 s	1024	1.23	0.181	0.44
		2048			0.44
		4096			0.43

Table 2: Overview on the impact of numerical and FFT parameters

NP is the number of FFT modes (or data points), ΔQ_{max} is the maximum peak-to-peak magnitude of the reactor power fluctuations and Sigma is the normalized root mean square magnitude (NRMS) of the fluctuations (both related to initial value and to 1K of temperature fluctuations).

The resonance frequency is practically independent from the numerical and FFT parameters. The maximum and the mean square magnitudes of the power fluctuations are determined not from the APSD spectrum, but from the power fluctuations calculated in the time domain. Therefore, they do not depend on the FFT parameters, but on the time step and the calculated process time. Comparing cases A, B and C, the magnitudes are the highest for case B, where the numerical diffusion is minimal. However, the impact of time step size is quite limited, because the numerical scheme used in DYN3D is low diffusive. In case D with longer process time we catch some additional higher power bursts than within 100 s.

The analysis of the variation studies has shown that calculations over a time interval of 100 s with a time step width of 0.05 s are optimal with respect to computation time and statistics. This time step width is in accordance with the Courant criterion. Although the statistics is improved increasing the calculated process time, for a qualitative estimation of the frequency behavior of the APSD and CCF, calculations over 100 s of process time are sufficient.

Summarizing the results from the calculation analysis of neutronic noise for uncorrelated fluctuations of the core inlet temperature we can state, that:

- The APSD both of local and global power fluctuations show a characteristic peak near a frequency of 0.5 Hz. This corresponds to results reported about in the literature e.g. (Runkel, 1987; Laggiard, 1997), where resonance frequencies between 0.5 and 1 Hz are mentioned. However, in the measurement data from the NPP, a dominating frequency of about 1 Hz was found.

- The NRMS of the global and local fluctuations of the reactor power/linear heat rate are very small (about 0.5 % per degree even for local fluctuations). However, relatively rare power bursts of up to 1.2 % K^{-1} for the global reactor power and 2.5 % K^{-1} for local power densities can be observed.
- The local neutronic signals show a phase shift corresponding to the transport time of the coolant through the FA.

The last feature is in contradiction to the measurement data from the power plants in a qualitative manner.

3.5 Correlated Temperature fluctuations

Physical model

Having in mind the results of the noise analysis caused by un-correlated temperature fluctuations at the core inlet, the question arises, if there could be mechanisms leading to fluctuations which could be, at least partially, correlated between the different fuel assemblies. This can be the case, if we consider fluctuations in the cold legs of the primary circuit loops. The fluctuation in one loop should have an impact on several FA in the core, because the mixing of the coolant in downcomer and lower plenum of a PWR reactor vessel is incomplete.

In the following, a physical model will be described, by the help of which correlated temperature fluctuations at the core inlet can be explained. This model is based on the following assumptions:

- The temperatures in the cold legs of the four primary loops show white noise fluctuations being independent from the fluctuations in each other loop. These fluctuations are assumed to be caused by physical and technical reasons in the components of the primary loops (steam generator, feedwater preheater etc.).
- The coolant temperature at the inlet of each fuel assembly, and therefore, also its fluctuating part, are determined by linear superposition of the cold leg temperatures of the loops corresponding to a so-called mixing matrix. This matrix contains the normalized portions of the coolant from each loop arriving at the inlet of the corresponding fuel assembly.
- The mixing matrix was obtained from experiments performed at the test facility ROCOM. ROCOM is a 1:5 scaled model of a PWR Konvoi with detailed geometrical modeling of the RPV and parts of the cold and hot legs. The mixing of the coolant was investigated by injecting a salt tracer and measuring its distribution at more than 1000 measurement points (Kliem, 2008; Kliem, 2008a).

Figure 13 shows the mixing matrix represented by the temperature distribution at the core inlet, if in one of the loops we have a higher temperature (arbitrarily by 5 K) than in the other loops.

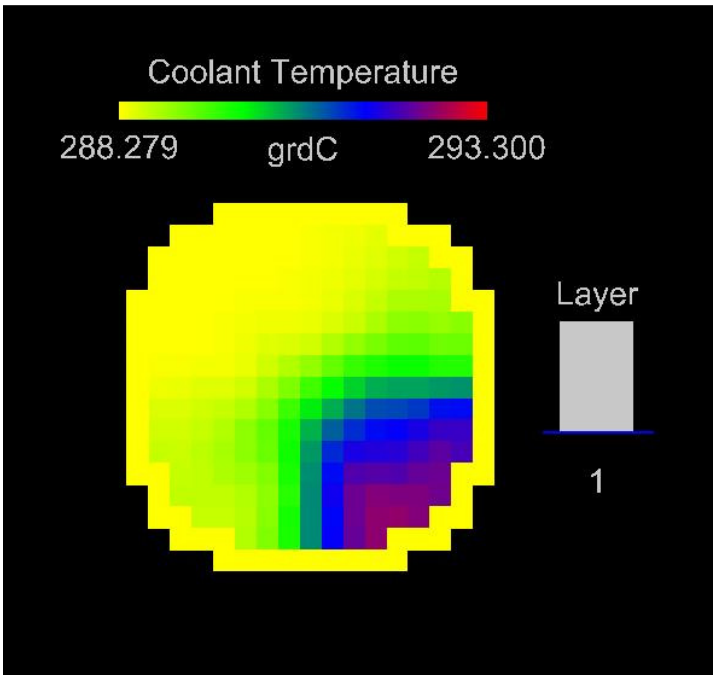

Fig. 13: Distribution of the coolant temperature at the core inlet for the case that the cold leg temperature in one of the loops is by 10 K higher than in the other ones

The temperature value T_k at each FA position k is calculated by the following formulas:

$$T_k(t) = \sum_{l=1}^{4} \xi_{k,l} T_l(t) \qquad \text{(Equ. 5)}$$

with $T_l(t) = T_0 + \Delta T \cdot (Z_l - 0.5)$ and $\sum_{l=1}^{4} \xi_{k,l} = 1$

where T_0 is the steady-state reference temperature, ΔT is the magnitude of the fluctuations, T_l are the loop temperatures, $\xi_{k,l}$ are the mixing coefficients from the matrix and Z_l is a random number between 0 and 1, which is selected for each time step and each FA statistically independent representing the white noise loop temperature fluctuations.

Figure 14 shows the numerical values of the mixing coefficients ξ_k, k = 1, 193 for loop number 1.

			0.000	0.000	0.002	0.007	0.012	0.020	0.032				
		0.000	0.000	0.000	0.000	0.003	0.009	0.016	0.025	0.041	0.059	0.072	
	0.000	0.000	0.000	0.000	0.000	0.004	0.011	0.022	0.037	0.054	0.072	0.079	0.098
	0.000	0.000	0.000	0.006	0.007	0.008	0.014	0.026	0.045	0.076	0.111	0.105	0.112
0.000	0.000	0.000	0.004	0.016	0.021	0.021	0.026	0.049	0.071	0.109	0.149	0.154	0.138	0.158
0.000	0.000	0.000	0.007	0.019	0.039	0.049	0.062	0.100	0.143	0.174	0.207	0.217	0.190	0.193
0.006	0.007	0.014	0.016	0.027	0.064	0.100	0.142	0.201	0.261	0.294	0.324	0.326	0.296	0.287
0.022	0.027	0.044	0.044	0.058	0.105	0.172	0.250	0.328	0.395	0.443	0.456	0.457	0.473	0.479
0.047	0.049	0.061	0.078	0.103	0.155	0.254	0.358	0.445	0.519	0.576	0.582	0.599	0.652	0.660
0.062	0.063	0.077	0.103	0.145	0.202	0.304	0.438	0.547	0.616	0.663	0.684	0.706	0.748	0.745
0.07	0.064	0.087	0.116	0.151	0.199	0.315	0.474	0.620	0.709	0.724	0.730	0.759	0.798	0.771
	0.071	0.083	0.110	0.127	0.164	0.303	0.486	0.662	0.783	0.792	0.779	0.812	0.817	
	0.082	0.079	0.083	0.100	0.147	0.281	0.489	0.693	0.817	0.847	0.845	0.842	0.820	
		0.075	0.074	0.094	0.157	0.312	0.491	0.669	0.818	0.865	0.867	0.852	
				0.104	0.168	0.305	0.493	0.681	0.812	0.864			

Fig. 14: Numerical values of the mixing matrix for loop number 1

Discussion of results

Figure 15 shows the APSD of the reactor power as a response to correlated temperature fluctuations. All calculations with correlated temperature fluctuations were performed assuming a magnitude of $\pm$ 5 K.

This is considered as a conservative estimate for the maximum magnitude of fluctuations. Assuming linearity, however, the magnitudes of the neutronic noise for comparison between different calculations can be related to a magnitude of fluctuations of 1K for normalization. The effective magnitude of the power fluctuations (NRMS) yields about 1.1 % of the reactor power per degree of temperature fluctuations, the maximum magnitude reaches 6.8 % K-1.

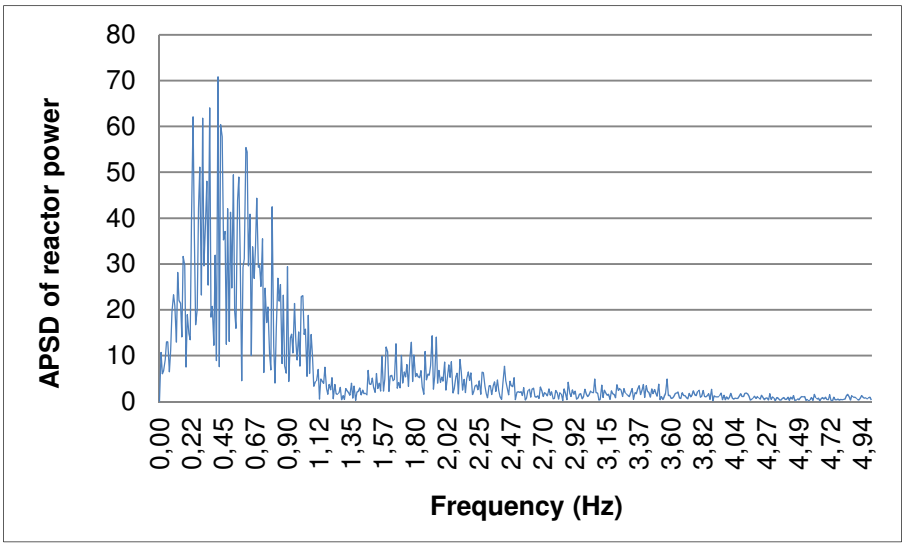

Fig. 15: APSD of the reactor power caused by temperature fluctuations in the primary loops

Figure 16 shows the APSD of the local linear heat rate (LHR) at three different positions in FA No 29. The average/maximum LHR is 39.2/28.9 kW/m. The LHR represent local neutronic signals.

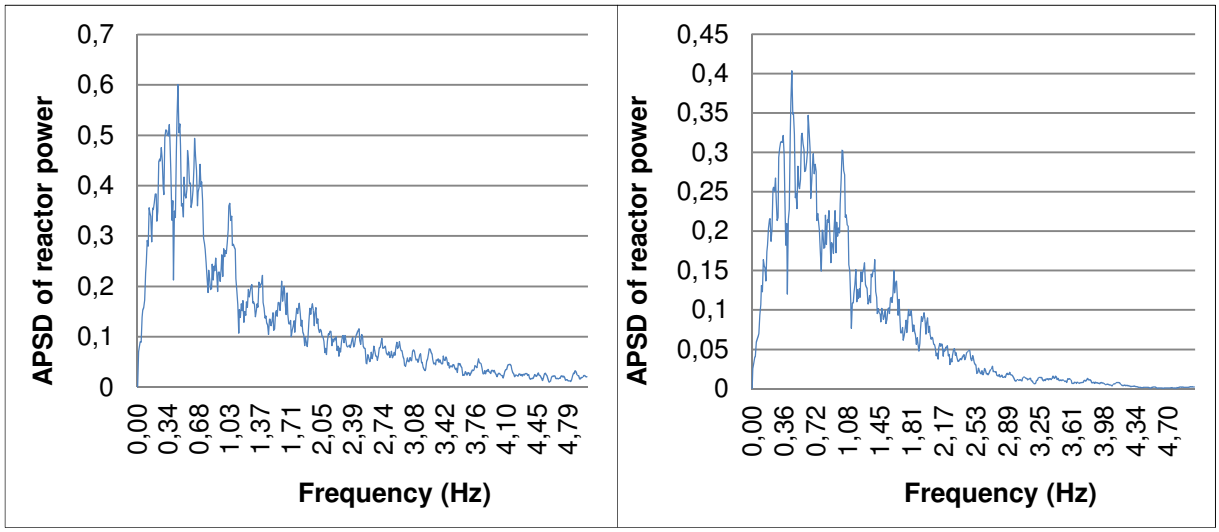

Figure 16: ASPDs in FA 29 smoothed and filtered in the frequency interval up to 5 Hz
left: at axial position z = 45cm, right: at z = 315 cm

The NRMS of the fluctuations in the lower and the upper part of the FA amount to about 1.65 and 1.5 % per degree of temperature fluctuation.

It can be stated, that the correlations between temperature fluctuations in different primary circuit loops, caused by incomplete mixing of the coolant in the downcomer and the lower plenum, cause a rise in the magnitude of the neutronic fluctuations by a factor of about 5-6 in the global and 4 in the local noise signals. The qualitative properties of the APSD functions are the same as for uncorrelated temperature-induced noise (resonance frequency, damping over height of the core, phase shift).

Correlation coefficients between local signals at the same axial position in different channels are high, if the channels are situated in the same core sector corresponding to a certain primary loop (e.g. 0.94 between FA No 29 and 41), but the correlations are also relevant between channels in different corners of the core (0.57 for FAs No 29 and 165) or even between local signals and the global reactor power (0.58 between core power and FA No 165). That means, global effects are relatively dominant in the case of correlated temperature fluctuations).

The NRMS of the local fluctuations indicate effective magnitudes of the neutronic noise of up to about 8 %, assuming conservative magnitudes of temperature fluctuations of 5 K. Such magnitudes have indeed been observed in some cases during the reactor operation.

As can be expected, the ratio between global and local neutronic fluctuations increases in the case of correlated temperature fluctuations, because parts of the core are connected, while in the case of uncorrelated fluctuations the contributions from the single fuel assemblies are more or less compensating each other.

The qualitative properties of the APSD functions are the same as for uncorrelated temperature-induced noise (resonance frequency, damping over height of the core, phase shift (Runkel 1987; Laggiard, 1997).

Therefore, the classical temperature induced neutronic noise can be excluded as an explanation for the observed power fluctuations.

In the next sections, we will consider more complex situations which can lead to local fluctuations of the neutron flux without the phase shift in the signals which is caused by the flow of the coolant through the cooling channel.

3.6 Fluctuations of the mass flow rate

Fluctuations of the coolant mass flow rate through the core also cause temperature and density fluctuations, but of different character like inlet temperature fluctuations. In the case of mass flow variations, the fluctuation of the core channel average temperature

$$(T_{av} + \delta T_{av}) = T_{in} + \frac{Q}{2(\dot{m}+\dot{\delta}\,\dot{m})c_p} \qquad \text{(Equ. 6)}$$

is given in first order approximation by $\delta T_{av} = \frac{Q}{2\dot{m}c_p}\frac{\delta\dot{m}}{\dot{m}}$

T_{av} is the average core temperature, Q the reactor power, $\dot{m}$ the core mass flow rate (without bypass flow) and c_p the average heat capacity corresponding to the core average temperature.

In our calculations we assumed uncorrelated mass flow fluctuations of $\pm$10 %. This corresponds to a magnitude of fluctuations of the core average coolant temperature of $\pm$1.7 K. For comparison with temperature induced noise we can scale again the neutronic fluctuations to 1 K of average core temperature fluctuation.

For simplicity, in steady state, the same mass flow rate will be assumed for each fuel assembly. In reality, there is some profiling of the mass flow rate over the channels due to different hydraulic characteristics. In PWR, this profiling is not so pronounced. For that reason, it can be neglected.

The fluctuations in the individual fuel assemblies are assumed to be statistically independent from each other. That means we consider uncorrelated mass flow fluctuations.

Fig.17 shows the APSD of the global reactor power in the case of uncorrelated mass flow fluctuations.

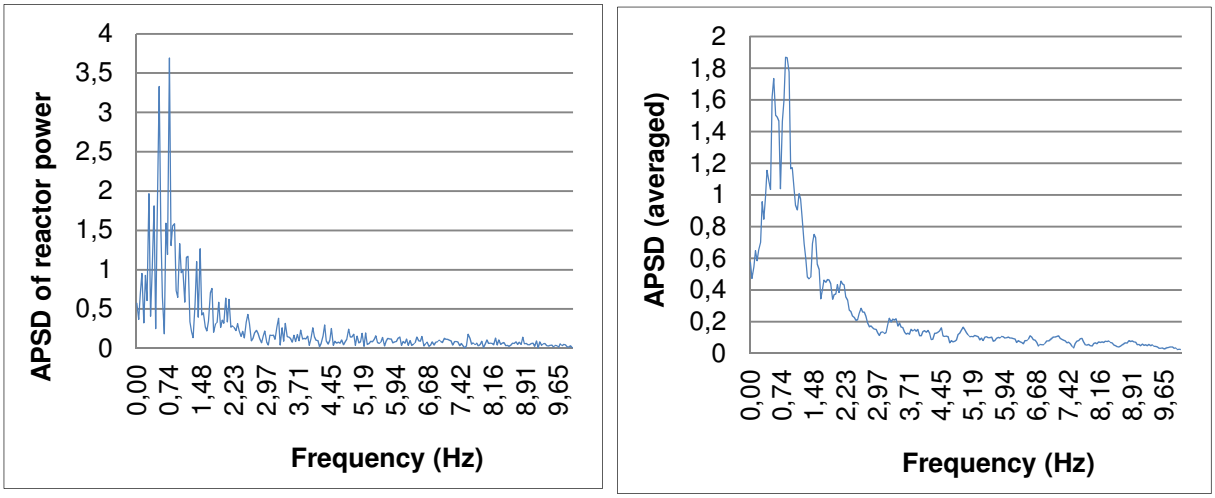

Fig. 17: APSD of the reactor power in the case of uncorrelated stochastic mass flow rate fluctuations
Left – unfiltered, right – smoothed

Fig. 18 shows the APSD of the local neutronic signals in FA No 29 at the axial positions z = 45 cm and z = 315 cm.

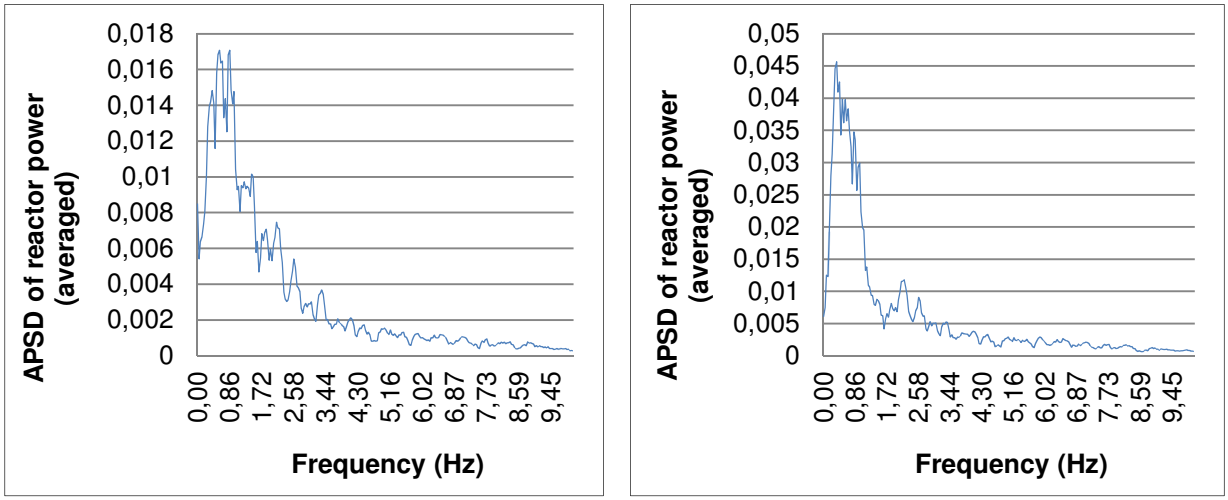

Fig. 18: APSD of the linear heat rate in the FA N^{o} 29
at the axial positions z = 45 cm (left) and z = 315 cm (right)

Different from the picture for noise induced by temperature fluctuations, for mass flow fluctuations, the magnitudes of the noise are about a factor of 2 higher in the upper part of the FA in comparison with the lower part. In the case of temperature induced noise we have seen a damping of the noise over the height of the core (see Fig. 6 and 7), while for mass flow fluctuations, the temperature fluctuations are rising with heat up of the coolant in the channels.

In the following, we consider again the cross correlations between noise signals at different heights of the cooling channel (see Fig. 19).

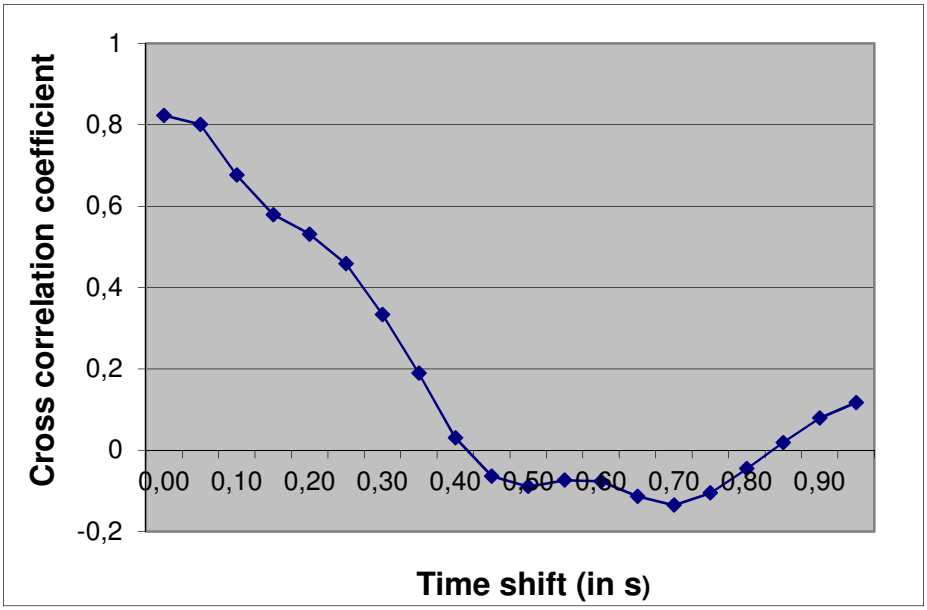

Fig. 19: CCF of the linear heat rate at axial positions z = 45 cm and z = 315 cm of the FA No 29

The cross correlation function shows high degrees of correlation for low time shift values and an almost perfect correlation for zero phase. That means, the neutronic noise signals are synchronous between the lower and upper part of the core. This can be explained by the fact, that temperature and moderator density fluctuations caused by mass flow variations, occur practically at the same time along the cooling channel. Mass flow variations proceed with velocity of sound, which amounts about 1000 m/s under the conditions in the reactor core.

The NRMS derived from the time curves are 0.1 % K^{-1} for the reactor power and maximum 0.3 % K^{-1} for the local signals. For the global reactor power, maximum magnitudes of about 0.5 % K^{-1} were obtained, for the local signals 1.5 % K^{-1}. Therefore, the magnitudes of the neutronic fluctuations in the case of mass flow rate variations are by about a factor of two less than in the case of fully stochastic temperature fluctuations. This is in accordance with results reported in (Bermejo, 2017). In contrast to the temperature fluctuations, the maximum of the local fluctuation is located in the upper part of the core.

The results of the analysis of mass flow fluctuations can be summarized as flows:

- A resonance region can be observed also in the case of mass flow rate fluctuations. However, the resonance frequency is shifted to slightly higher frequencies (0.6 – 0.8 Hz).
- The phase shift between noise signals over the height of the coolant channels, which is characteristic for temperature induced noise is missing in noise caused by mass flow rate fluctuations. The noise signals in the upper and the lower part of the core are practically synchronous, as it was observed in the measurements.
- In temperature induced neutronic noise, the noise signals are damped over the height of the cooling channel, while they are growing in the case of noise caused by mass flow rate fluctuations.
- The magnitudes of neutronic noise obtained in the simulations, can reach maximum 1.5 % per degree of equivalent temperature fluctuation for local signals. This is too low in comparison with observations on plants. Magnitudes of mass flow fluctuations of more than 10 % as assumed in the simulations are likely improbable.

3.7 Fluctuations of the moderator density

Model and boundary conditions

Besides of neutronic noise induced by coolant inlet temperature fluctuations or fluctuations of the mass flow rate, simulations of neutronic noise were performed, which is caused by direct generic fluctuations of the moderator density. It was assumed, that in a part of the reactor core the moderator density undergoes homogeneously distributed, uncorrelated stochastic fluctuations. These simulations were aimed to investigate the transfer behavior of fluctuating moderator density to the neutronics outside the chain of thermo-hydraulic feedback.

The moderator density was stochastically varied in each node of an axial core region in the range between 135 cm and 280 cm of the active core height. This assumption is based on the idea, that the effective water content in the fuel grid or local fuel/moderator ratio is fluctuating caused by any external reasons outside the thermal hydraulics, e.g. by mechanical vibrations of the fuel rods. The change in local fuel/moderator ratio was modeled by changing the moderator density. Such fluctuations show maximum magnitudes in the middle of the core, assuming that the fuel rods are fixed at the top and the bottom.

Movements of fuel rods and, in general, changes in local geometry of the core nodes, cannot be modelled in DYN3D. Therefore, direct fluctuations of the macroscopic cross sections were assumed, which are obtained according to fluctuations of the moderator density. The density fluctuations were assumed as white noise.

To generate varying cross sections corresponding to moderator density fluctuations, a special procedure was implemented into DYN3D, interpolating the cross sections from a pre-calculated data library. The moderator density values used in the lattice code calculations were varied by ±12 kg/m^3 what corresponds to a magnitude of temperature fluctuations of ±5 K. The actual density value is determined stochastically, and the cross sections are interpolated from the library in accordance with the chosen density. These fictive density variations have an impact only on the neutron kinetics, they are not connected with violations of the mass, energy and momentum balance of the coolant fluid.

Fig. 20 shows the moderator density fluctuations over time in one of the core nodes.

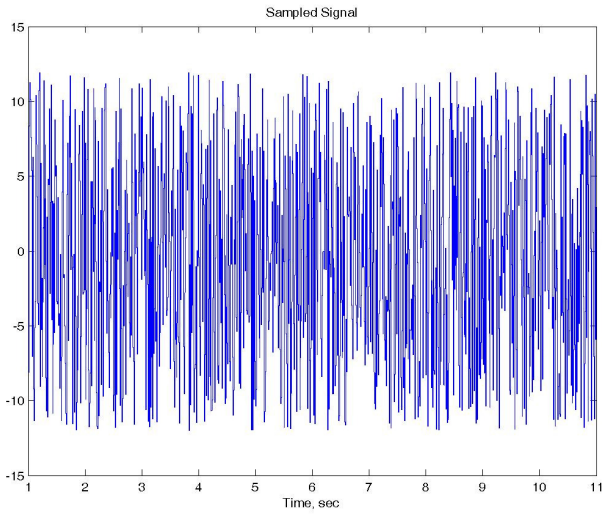

Fig. 20: Local density fluctuation over time at axial position z = 190 cm in FA No 151

Results of the simulations

Figure 21 shows the variation of the reactor power caused by neutron cross section variations due to fluctuating moderator density.

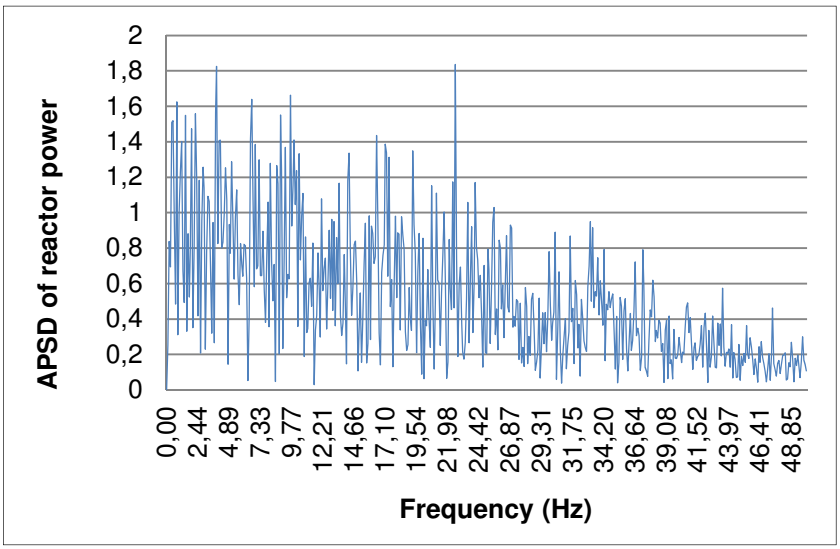

Fig. 21: APSD of the reactor power caused by stochastic fluctuations of the cross sections depending from moderator density

Different from the temperature induced noise, we do not observe a resonance of the APSD at low frequency. The spectrum of the APSD is much broader. We observe relevant magnitudes even at frequencies higher than 30 Hz. This can be explained by the fact, that no filtering of the input noise by thermo-hydraulics is performed.

Concerning the maximum peak-to-peak magnitude of the reactor power fluctuation and the NRMS of the fluctuations, derived from the power signal in time domain, we obtain 0.3 % rsp. less than 0.1 % related to 1K of equivalent temperature fluctuation.

The APSD of the linear heat rate at different axial positions of the hottest FA are shown in Fig. 22. It must be noted, the subdivision of the FA into axial layers in the calculations with density variations was different from the basic calculations. A number of 32 nodes with a height of 12.2375 cm each were used.

As for the global reactor power, the maximum and NRMS magnitudes of the local noise signals, related to 1 K, are lower as for uncorrelated temperature fluctuations. The maximum magnitude for node number 21 (at height of 226 cm from the core bottom) amounts about 1.3 % K^{-1}, for node number 10 (at height of 92 cm) only 0.5 % K^{-1}. The mean square fluctuations are 0.3 % K^{-1} and about 0.1 % $K^{-1,}$ correspondingly.

The density perturbations are limited to the axial layers from No 13 to 24. This corresponds to 37 % of the core height. Node No 10 is situated below the perturbation zone. The noise observed in this region is partially induced by global effects, partially by local components decaying with the distance from the perturbation zone. Node No 21 is located within the perturbation zone. That's why the APSDs of the local neutronic signals are higher than in node No 10.

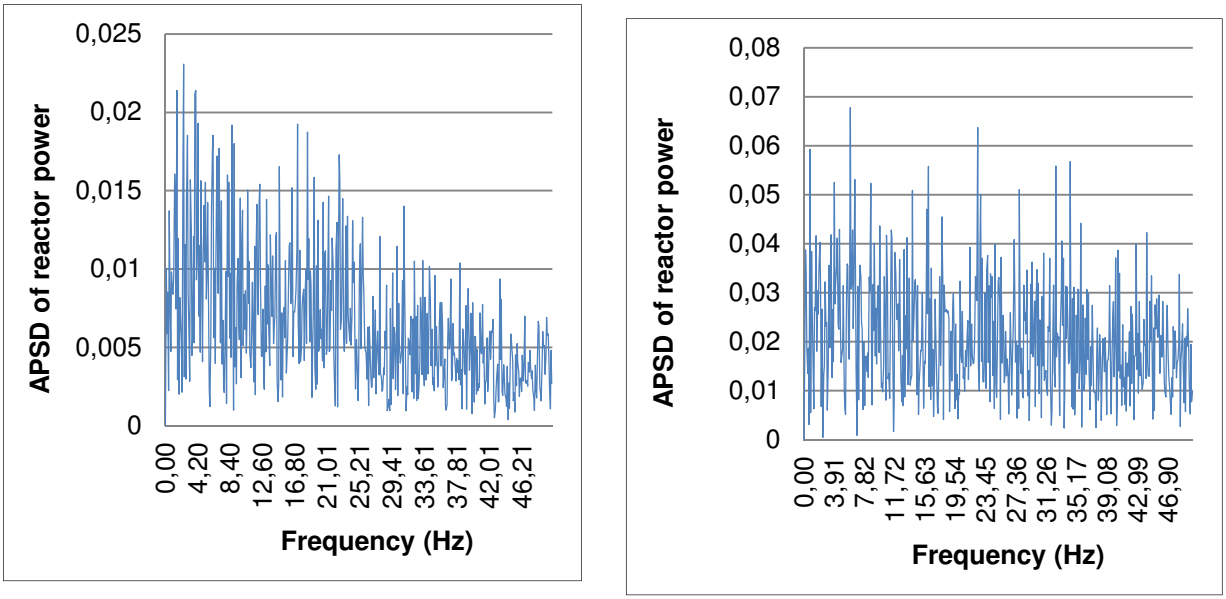

Fig.22: APSD of the linear heat rate in FA No 29
left: axial layer 10 (z = 92 cm), right: axial layer 21 (z = 226 cm)
Axial positions measured from the bottom of the core

The cross correlation functions of the local noise signals at different axial positions in FA No 29 are shown in Fig. 23. The nodes 16 and 21 are both located in the perturbation area. The neutron flux fluctuations at these two positions are only slightly correlated (see upper part of Fig. 24). The fluctuations in these nodes are determined mostly by local density variations which are statistically independent. Nodes 10 and 12 are situated below the perturbation region. The APSD in node 10 is about a factor of 3 lower than in node 21. However, the local signals from nodes 10 and 12 are strongly correlated at zero phase shift. That means, they are nearly synchronous. This is because the noise outside the perturbation zone is stronger influenced by the global reactor noise.

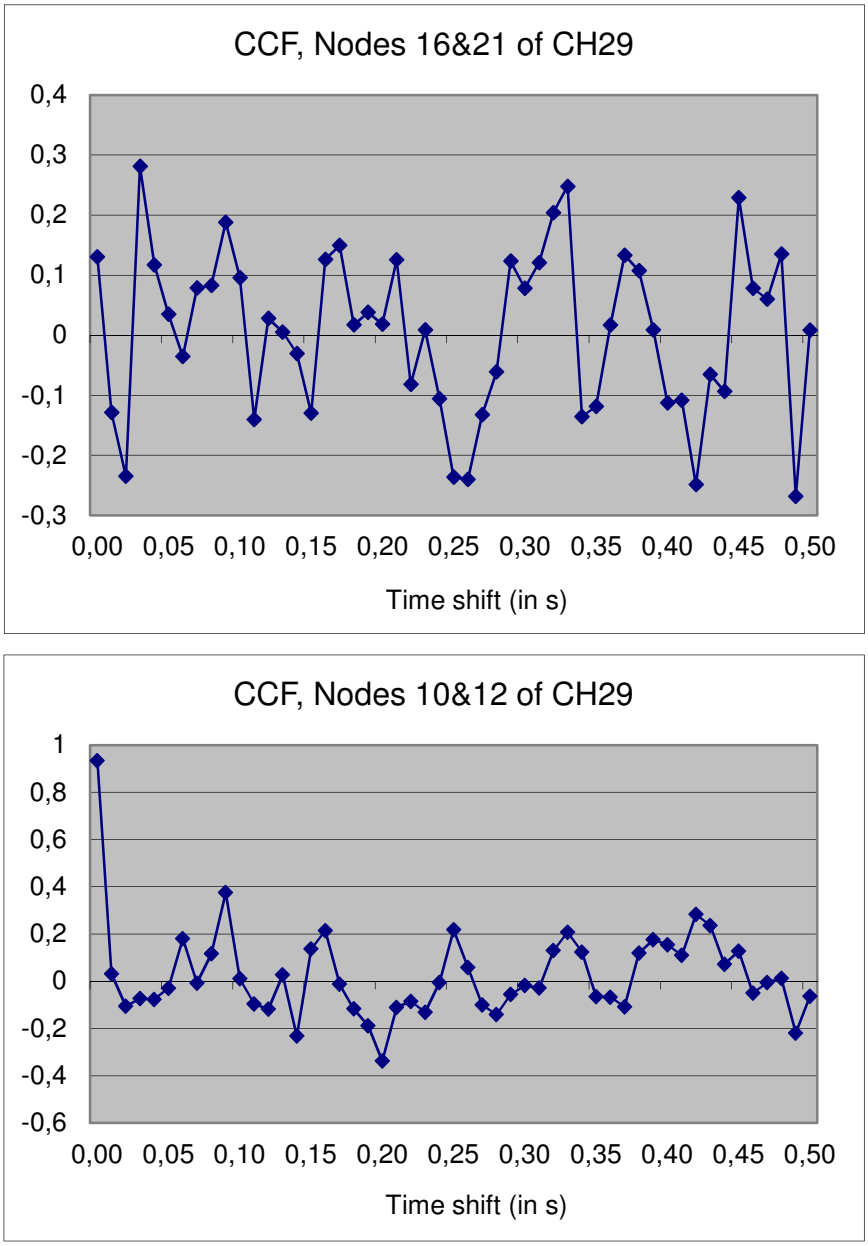

Fig. 23: Cross correlation functions between the signals from nodes 16 und 21 (above) as well as 10 and 12 (below)

Summarizing the results of density fluctuation simulations we can conclude the following:

- Related to one degree of equivalent temperature fluctuation, the effective magnitudes of global reactor power fluctuations are less than 0.1 %, for local fluctuations of about 0.25 %. The maximum magnitudes of local fluctuations reach about 1.3 % K^{-1}.
  One degree of temperature fluctuations is equivalent to about 2.4 kg/m³ of density variation that means of about 0.4 % of the average moderator density. Considering mechanical vibrations of the fuel rods, which can lead in extreme case to vanishing gap between neighboring rods, the fuel/moderator relation can change locally (in the vicinity of one rod) by 30-40 %, may be, a few percent in a region of a FA. One can imagine that this could lead to local noise magnitudes in the order of 10 %, as it was observed in the measurements.

- The “density induced” noise shows no phase shift between signals from locations at different axial positions, as it is clearly expressed for temperature induced noise. This corresponds to observations, too.
- The spectrum of the density induced noise is much broader than the spectrum of temperature induced noise. A characteristic peak, as the 0.5 Hz peak in temperature induced noise, does not exist. While the APSD of the temperature induced noise is decaying very quickly above the peak, in the APSD of density induced noise we have relevant contributions even above 30 Hz.
- The density fluctuations were assumed as white noise. The impact of eigen-frequencies of mechanical vibrations was not considered. These frequencies should be visible in the APSD spectrum of the neutronic noise.

It is clear, that the assumptions and simplifications made in the simulations of neutronic noise, caused by moderator density fluctuations due to impacts outside of the core thermal hydraulics do not allow drawing final conclusions. More complex simulations are necessary, including neutronics coupled with thermal hydraulics, mechanical models and CFD.

4. Summary on DYN3D simulations

In this section, an overall summary of the results of DYN3D simulations of neutronic noise caused by coolant inlet temperature variations, variations of the channel-wise massflow rate and the local moderator density in a part of the core is given. Numerical results are compiled in table 3. Approximate values of parameters are given having in mind that these values do have statistical uncertainties.

Perturbation type	NRMS magnitude global/local (% K^{-1})	Maximum magnitude global/local (% K^{-1})	Frequency behavior	Resonance frequency (Hz)	Time shift over channel height (s/m)
Temperature stochastic	0.20/0.4	1.1/2.3	Sharp resonance	0.45	0.2
Temperature correlated	1.1/1.65	7/10	Sharp resonance	0.45	0.2
Mass flow rate	0.1/0.3	0.5/1.5	Maximum	0.8	no
Local moderator density	0.1/0.2	0.3/1.3	Broad band	-	no

Table 3: Characteristic parameters of the neutronic noise for different kinds of fluctuations

Based on table 3, the following characteristics of the simulated neutronic noise can be given:

Magnitudes of neutronic fluctuations

In the case of fully stochastic temperature or mass flow rate fluctuations, the magnitudes of both local signals and global reactor power noise are lower than it was observed in Konvoi type PWR. Related to one degree of equivalent temperature fluctuation, the magnitudes for mass flow fluctuations are about two times lower than for temperature induced noise.

In the case of correlated temperature fluctuations, which are derived from cold leg temperature variations in the primary loops, magnitudes of about 10 % as observed in some reactors can be reached.

Fluctuations of the local moderator density or, equivalently, the moderator content in the fuel cells, could have the potential to cause neutronic noise of relevant magnitudes.

Frequency behavior

The APSD spectrum of temperature induced noise signals show a well pronounced maximum at a frequency of about 0.5 Hz. Above this resonance frequency, the APSD decreases very quickly. The same behavior was observed for noise induced by mass flow variations. However, in this case we have obtained a little bit higher resonance frequencies.

In the case of moderator density variations, broad band spectrum APSD without explicit resonance were obtained. If we assume mechanical vibrations within the FA as a reason for the water density fluctuations, an impact of the eigenfrequencies of these mechanical vibrations on the APSD spectrum has to be expected.

Cross correlations

Cross correlations analyses of the neutronic signals from different locations have shown a phase shift over the height of the coolant channels for temperature induced noise. This phase shift corresponds to the transport time of the coolant along the channel and is well known from the literature. However, such kind of phase shifts has not been detected in the measurement signals.

High correlation coefficients (about 0.9) have been obtained between FA in the same core sector related to a certain primary circuit loop for correlated temperature fluctuations. Significant correlation coefficients (about 0.6) were found between local and global signals, what indicates an important part of global noise.

5. OUTLOOK ON THE USE OF NEW CORE SIMULATION TOOLS

Code coupling has seen an enormous interest in recent years. The main emphasis has been the coupling between thermal-hydraulic codes for system analysis with 3D neutronic codes for reactor core power calculations (e.g. Beam, 1999; Hämäläinen, 2002; Kereszturi, 2003; Kozmenkov, 2015; Uvakin, 2016). Additionally, CFD or sub-channel codes have been used for a detailed core thermal-hydraulic analysis in connection with 3D neutronic codes (e.g. Gomez-Torres, 2012; Kliem, 2011, Grahn, 2015). Furthermore attempts have been made to couple fuel performance codes with neutronic codes (Bascou, 2015; Holt, 2015; Holt, 2016).

On the other hand of the spectrum there have been a number of efforts to simulate the detailed in-core coolant flow under steady-state conditions with CFD tools (e.g. Krepper, 2007; Krepper 2012; Kochunas, 2012).

Missing in this series of efforts is the coupling between the fuel assembly thermo-mechanical behavior, the neutron field and the coolant flow as a function of time. As an intermediate step there have been a number of publications addressing the prediction of fuel assembly bow under reactor conditions (e.g. Stabel, 2011; Horvath, 2013).

To better understand the neutron noise the above mentioned new coupling approach is necessary for the following reason: the recently observed increase and decrease of neutron noise in Germany's KWU type of plants was not accompanied by any specific increase or decrease at a certain frequency of the ASPD, but by a broadband increase and decrease of the LFNS (Seidl, 2015). According to the classical picture this would imply an increase or decrease of the inlet moderator temperature fluctuations. This is not plausible since the

primary circuit remained unchanged. On the other hand this period is in coincidence with the use of fuel assemblies with weaker and stronger lateral stiffness, respectively. This indicates that there may be a more sophisticated root cause for the LFNS.

In order to accomplish this more advanced coupling a number of developments are necessary. First of all the time dependent behavior of the inlet mass and temperature fluctuations under steady state conditions need to be calculated, i.e. the frequency distribution of the core inlet parameters under normal operating conditions. This can be achieved in principle by using CFD tools with their time-dependent solver under steady state conditions. However the computational efforts would still require many millions of CPU hours and would need to be done at a national super-computer research center.

Second, the time dependent response of the mechanical fuel assembly structure in full core geometry needs to be calculated by utilizing the above mentioned time dependent core inlet boundary conditions. A feedback between fuel assembly mechanical response and in-core moderator flow can possibly be neglected in zero order attempts because the fuel assembly movements are expected to be small compared to core-wide flow patterns.

Finally this then would need to go hand in hand with simulations of the time behavior of the dynamic fuel-to-moderator changes affecting the core's neutronic response. This could be accomplished with established codes which are already capable of simulating fuel-to-moderator by pre-calculated cross section changes as a function of fuel to fuel assembly and pin to pin pitches. A coupling with fuel performance codes would not be necessary because of the comparatively long time constant of the fuel pellets' thermal response compared to the observed variations in neutron noise.

At the end of this series of calculations would stand a prediction of the neutron noise response to given fluctuating inlet core boundary conditions. This may lead to two outcomes: it may turn out that to the best of knowledge fluctuations of the inlet core parameters may be too small and the fuel assembly stiffness to big in general to cause any noticeable contribution to the neutron noise. These calculations may also answer the question how big the inlet core parameters need to change or fluctuate to be considered a primary reason for the magnitude of the neutron noise. The other outcome may be that under steady state condition core inlet parameters with regard to mass flow and temperature fluctuations and just in the right order of magnitude to be considered the root cause of neutron noise in Germany's KWU built reactors.

LIST OF ABBREVIATIONS

APSD Auto-Power Spectral Density
CCF Cross Correlation Function
FA Fuel Assembly
FFT Fast Fourier Transformation
LFNS Low Frequency Neutron Noise
LHR Linear heat rate
NRMS Normalized Root Mean Square
PWR Pressurized Water Reactor

REFERENCES

Bascou, S., De Luze, O., Ederli, S., Guillard, G., Development and validation of the multi-physics DRACCAR code, Annals of Nuclear Energy, 84, 1 (2015)

Beam, T. M., Ivanov, K. N., Baratta, A. J., Finnemann, H., Nodal kinetics model upgrade in the Penn State coupled TRAC/NEM codes, Annals of Nuclear Energy 26, 1205 (1999)

Bermejo, J.A.; C. Montalvo, A. Ortego, On the possible effects contributing to neutron noise variations in KWU-PWR reactor: Modelling with S3K, Progress in Nuclear Energy 95, 1 (2017)

Bilodid, Y., Kotlyar, D., Shwageraus, E., Fridman, E., Kliem, S., Hybrid microscopic depletion model in nodal code DYN3D. Annals of Nuclear Energy, 92, 397 (2016)

Bläsius, Ch.; J. Herb and M. Küntzel, Untersuchungen der Ursachen für Neutronenflußschwankungen, Garching, January 2016, ISBN 978-3-944161-90-7

Cooley, J.W., Tuckey J.W., An algorithm for the machine calculation of complex Fourier series, Mathematics of Computation, 19, 297 (1966)

Debevec, P.T., The Excel FFT Function v1.1, http://blogs/epfl/ch/document/11828 (2006)

DIN 25475-2:2009-05, Nuclear facilities - Operational monitoring - Part 2: Vibration monitoring for early detection of changes in the vibrational behavior of the primary coolant circuit in pressurized water reactors, Deutsches Institut für Normung e.V. (2009)

Duerigen S., Rohde, U., Bilodid, Y, Mittag, S., The reactor dynamics code DYN3D and its trigonal-geometry nodal diffusion model, Kerntechnik, 78, 310 (2013)

Fiedler, J., Schwingungsüberwachung von Primärkreiskomponenten in Kernkraftwerken (Doctoral Dissertation), University Hannover (2002)

Gomez-Torres, A. M., Sanchez-Espinoza, V. H., Ivanov, K., Macian-Juan, R., DYNSUB: A high fidelity coupled code system for the evaluation of local safety parameters – Part I: Development, implementation and verification, Annals of Nuclear Energy, 48, 108 (2012)

Grahn, A., Kliem, S., Rohde, U., Coupling of the 3D neutron kinetic core model DYN3D with the CFD software ANSYS-CFX, Annals of Nuclear Energy, 84, 197 (2015)

Grondey, G., et al., Low frequency noise in a PWR and its influence on the normal operational characteristics of the plant. In: Specialists' Meeting on Incore Instrumentation and Reactor Core Assessment, Pittsburg, PA, pp. 183-191 (1992)

Grundmann, U., Hollstein, F., A two-dimensional intranodal flux expansion method for hexagonal geometry, Nuclear Science and Engineering, 133, 201 (1999)

Grundmann, U.; U. Rohde, S. Mittag, S. Kliem: DYN3D Version 3.2, Code for Light Water Reactors (LWR) with Hexagonal or Quadratic Fuel Elements, Description of models and methods, Technical Research Report FZR-434, ISSN 1437-322X (2005)

Hämäläinen, A., Kyrki-Rajamäki, R., Mittag, S., Kliem, S., Weiß, F.-P., Langenbuch, S., Danilin, S., Hádek, J., Hegyi, G.,. Validation of coupled neutron kinetic/thermal-hydraulic codes, Part 2: Analysis of a VVER-440 transient (Loviisa-1). Annals of Nuclear Energy, 29, 255 (2002)

Holt, L., Rohde, U., Seidl, M., Schubert, A., Van Uffelen, P., Macián-Juan, R., Development of a general coupling interface for the fuel performance code TRANSURANUS – Tested with the reactor dynamics code DYN3D, Annals of Nuclear Energy, 84, 73 (2015)

Holt, L., Rohde, U., Kliem, S., Baier, S., Seidl, M., Macían-Juan, R., Investigation of feedback on neutron kinetics and thermal hydraulics from detailed online fuel behavior modelling during a boron dilution transient in a PWR with the two-way coupled code system DYN3D-TRANSURANUS, Nucl. Eng. Design, 297, 32 (2016)

Horvath, A., Dressel, B., On numerical simulation of fuel assembly bow in pressurized water reactors, Nucl. Eng. Design, 265, 814 (2013)

Keresztúri, A., Hegyi, G., Marázcy, C., Panka, I., Telbisz, M., Trosztel, I., Hegedüs, C., Development and validation of the threedimensional dynamic code—KIKO3D, Annals of Nuclear Energy, 30, 93 (2003)

Kerr, D. A., The Fourier Analysis Tool in Microsoft Excel (2009), http://dougkerr.net/Pumpkin/articles/Excel_Fourier.p

Kochunas, B. et al., Coupled full core neutron transport/CFD simulations of pressurized water reactors, In Proc. of PHYSOR 2012 (2012)

Kliem, S., Rohde, U., Weiss, F.-P., Core response of a PWR to a slug of under-borated water, Nuclear Engineering and Design, 230, 121 (2004)

Kliem, S.; Suehnel, T.; Rohde, U.; Hoehne, T.; Prasser, H.-M.; Weiss, F.-P., Experiments at the mixing test facility ROCOM for benchmarking of CFD-codes, Nuclear Engineering and Design 238, 566 (2008)

Kliem, S., Prasser, H.-M., Suehnel, T., Weiss, F.-P., Hansen, A., Experimental determination of the boron concentration distribution in the primary circuit of a PWR after a postulated cold leg small break loss-of-coolant-accident with cold leg safety injection, Nucl. Eng. Design, 238, 1788 (2008a)

Kliem, S., Gommlich, A., Grahn, A., Rohde, U., Schütze, J., Frank, T., Gomez, A., Sanchez, V., Development of multi-physics code systems based on the reactor dynamics code DYN3D, Kerntechnik, 76, 160 (2011)

Kliem, S., Bilodid, Y., Fridman, E., Baier, S., Grahn, A., Gommlich, A., Nikitin, E., Rohde, U., The reactor dynamics code DYN3D, Kerntechnik, 81, 170 (2016)

Krepper, E., Koncar, B., Egorov, Y., CFD modelling of subcooled boiling-Concept, validation and application to fuel assembly design, Nuclear Engineering and Design, 237, 716 (2007)

Krepper, E., Rzehak, R., CFD Analysis of a Void Distribution Benchmark of the NUPEC PSBT Tests: Model Calibration and Influence of Turbulence Modelling, Science and Technology of Nuclear Installations, 939561 (2012)

Laggiard, E., Runkel, J., Evaluation of the Moderator Temperature Coefficient of Reactivity in a PWR by Means of Noise Analysis, Ann. Nucl. Energy 24 (1997) 411-417

Liewers, P., Rauschdiagnostik, Akademie-Verlag, Berlin, 1985

Richtmyer, R.D. and K. W. Morton, Difference Methods for Initial-Value Problems, Interscience Publishers, New York - London - Sydney, 1967

Robinson, J. C., Analysis of neutron fluctuation spectra in the Oak Ridge Research Reactor and the High Flux Reactor, ORNL-4149 (1967)

Rohde, U., The modelling of fuel rod behaviour under RIA conditions in the code DYN3D, Annals of Nucl. Energy 28, 1343 (2001)

Rohde, U.; Kliem, S.; Grundmann, U.; Baier, S.; Bilodid, Y.; Duerigen, S.; Fridman,E.; Gommlich, A.; Grahn, A.; Holt, L.; Kozmenkov, Y.; Mittag, S.: The reactor dynamics code DYN3D – models, validation and applications, Progress in Nuclear Energy, 89, 170 (2016)

Runkel, J., Noise Analysis in Pressurized Water Reactors (Doctoral Dissertation), 1987

Seidl, M. Kosowski, K., Schüler, U., Belblidia, L., Review of the historic neutron noise behavior in German KWU built PWRs, Progress in Nuclear Energy, 85, 668 (2015)

Stabel, J., et al., Advanced methodology to predict in-reactor bow of PWR fuel assemblies for efficient design optimization: background, validation, examples. In: Proceedings 2011 Water Reactor Fuel Performance Meeting, Chengdu, China, Sept. 11-14, 2011

Uvakin, M. A., Alekhin, G. V., Bykov, M. A., Zaitsev, S. I., Verification of three-dimensional neutron kinetics model of TRAP-KS code regarding reactivity variations, Kerntechnik, 81, 394 (2016)

Weinberg, A. and Schweinler, H., Theory of oscillating absorber in a chain reactor. Phys. Rev. 78 (8), 851 (1948)